International Journal of Automotive Technology, Vol. 18, No. 4, pp. 571−578 (2017)
DOI 10.1007/s12239−017−0057−x

pISSN 1229−9138/ eISSN 1976−3832

REDUCTION OF ENGINE EMISSIONS VIA A REAL-TIME ENGINE COMBUSTION CONTROL WITH AN EGR RATE ESTIMATION MODEL

Seunghyun Lee[1)], Hoimyung Choi[2, 3)] and Kyoungdoug Min[1)*]

[1)]Department of Mechanical and Aerospace Engineering, Seoul National University, Seoul 08826, Korea
[2)]Advanced Institutes of Convergence Technology, 145 Gwanggyo-ro, Yeongtong-gu, Suwon-si, Gyeonggi 16229, Korea
[3)]Department of Mechanical Engineering, Gachon University, Gyeonggi 13120, Korea

(Received 30 August 2016; Revised 13 December 2016; Accepted 6 January 2017)

ABSTRACT−Vehicle emissions regulations are becoming increasingly severe and remain a principal issue for vehicle manufacturers. Since, WLTP (Worldwide harmonized Light vehicles Test Procedures) and RDE (real driving emission) regulations have been recently introduced, the engine operating conditions have been rapidly changed during the emission tests. Significantly more emissions are emitted during transient operation conditions compared to those at steady state operation conditions. For a diesel engine, combustion control is one of the most effective approaches to reduce engine exhaust emissions, particularly during the transient operation. The concern of this paper is about reducing emissions using a closed loop combustion control system which includes a EGR rate estimation model. The combustion control system calculates the angular position where 50 % of the injected fuel mass is burned (MFB50) using in-cylinder pressure for every cycle. In addition, the fuel injection timing is changed to make current MFB50 follow the target values. The EGR rate can be estimated by using trapped air mass and in-cylinder pressure when the intake valves are closed. When the EGR rate is different from the normal steady conditions, the target of MFB50 and the fuel injection timing are changed. The accuracy of the model is verified through engine tests, as well as the effect of combustion control. The peaks in NO level was decreased during transient conditions after adoption of the EGR model-based closed loop combustion control system.

KEY WORDS : EGR estimation, Model-based control, Closed-loop control, Exhaust emission transient condition

NOMENCLATURE

A : area, m^2
ATDC : after top dead center
BDC : bottom dead center
BMEP : brake mean effective pressure
CA : crank angle
CI : compression ignition
ECU : electric control unit
EGR : exhaust gas recirculation
IVC : intake valve close
PM : particular matter
RGF : residual gas fraction
SOC : start of combustion
BTDC : before top dead center

SUBSCRIPTS
c : convective
RG : residual gas
HT : heat transfer
no HT : without heat transfer
p : piston
press : pressure

**Corresponding author.* e-mail: kdmin@snu.ac.kr

1. INTRODUCTION

Each continent annually introduces strict emission legislation and discusses an even stricter emission legislation roadmap for the long term. This stricter legislation increases the pressure on automotive companies. For example, the Tier 2/Bin 5 regulation in the US restricts NOx and PM emissions to 0.043 g/km and 0.006 g/km, respectively. For a diesel engine, reducing both the NOx and PM emissions requires intensive research because they have a trade-off relationship. The current emissions legislation in Europe, Euro 6, restricts PM emissions to 0.003 g/km and NOx emissions by 0.08 g/km (Guillemin *et al*., 2008; Punater *et al*., 2008).

Transient engine operation is a significant source of regulated exhaust emissions; therefore, the nature of this emission formation must be more closely investigated. Swain et al. described a method to compare emissions from transient state with emissions from steady state and showed that NOx, HC, and PM emissions were emitted 8 %, 42 %, and 60 % more, respectively, in the transient state compared to in steady state. Kang *et al*. (2005) investigated

the behavior of NO and HC emissions in transient state with fast response emission analyzers by increasing torque at constant speed and increasing speed at constant torque with changing injection timing end EGR rate. The result showed that the highest peak NOx emissions occurred for step load changes. Hagena *et al*. (2006) investigated characteristics of NO and PM emissions during a tip-in procedure by changing the ramp time of the transient operation. The results showed that when ramp time was shorter, more emissions were emitted. The NOx peak was 1.8 times higher and PM peak was more than 10 times higher. Both NOx and PM emissions were characterized by a significant increase in instantaneous emission levels as the ramp-up time was reduced. The primary reason for the change in NOx was due to the lag between increased fuel demand and the response of the air-charging system as well as EGR starvation during the initial phase. The injection pressure and exhaust pressure history have a secondary impact on emissions. For PM, the initial part of the transient state initiated by the step change in fuel demand appeared to be critical. The lack of air due to turbo lag, poor mixing, increased wall impingement and the surplus of EGR at the very beginning of the event were responsible for the change in fuel demand (Kirchen *et al*., 2009; Hagena *et al*., 2006; Kang and Farrell, 2005).

An open-loop control method has been selected to adjust the parameters related to the operating variables in the traditional control system of diesel engines. In the open loop control system, the values of the operating parameters are determined by only engine operation conditions without feedback. Thus, this open-loop control system has no inherent ability to compensate for undesired engine conditions caused by transient operations such as the air and EGR system delay. However, a closed-loop control system that measures results of the actual combustion has the ability to include environmental factors and has advantages for on-board diagnostics (Yoon *et al*., 2007; Ohyama, 2001).

Closed-loop combustion control was introduced to reduce engine emissions, compensate for changes in external conditions or fuel characteristics and to acquire stable engine operation for low temperature combustion engines (Reitz and Ehe, 2006; Hasegawa *et al*., 2006; Husted *et al*., 2007; Kumar *et al*., 2007; Schnorbus *et al.*, 2008; Liebig *et al*., 2008; Willems *et al*., 2010). Many automotive manufacturers have also been interested in engine control based on cylinder pressure (Audi Diesel Targets Bin 5, Euro 6, 2015; Honda Prepares i-DTEC Diesel for 2009, 2015; New GM V6 Diesel Has Cylinder-pressure Monitoring, 2015; VW Jetta SportWagen Scores High, 2008).

Yoon *et al*. (2007) performed a study to control SOC (start of combustion) in a diesel engine. The SOC was calculated using in-cylinder pressure and controlled by the feedforward controller. Their results show that the cylinder by cylinder SOC variation was effectively reduced (Yoon *et al*., 2007).

Liebig *et al*. (2008) investigated effects of closed loop control system with fuel variation. When the diesel engine was controlled by closed loop, the ignition quality was improved. Moreover, NOx and PM emissions were reduced in comparison to the open loop control, though the cetane numbers of the fuels varied from 55 to 39 (Liebig *et al*., 2008).

Yu *et al*. (2013) investigated the closed control method using MFB50 feedback. The current MFB50 driven from in-cylinder pressure data in real time was controlled to follow targets, which were determined from steady state experiments. The results showed that the closed loop control was effective in reducing PM in NEDC mode (Yu *et al*., 2013).

It is essential for the real-time engine control to account for the state of the in-cylinder cycle by cycle. However, there is little concern for the in-cylinder gas composition and its relationship to combustion control, even though the in-cylinder gas composition is one of the most important concerns related to the in-cylinder. This composition has a significant effect on in-cylinder combustion and exhaust emissions. Therefore, combustion control logic that considers the EGR rate of each cylinder is required to reduce exhaust emissions. In this research, a real-time EGR rate estimation model was developed. Then, the estimated EGR rate was used to control the engine cycle by cycle and cylinder to cylinder to reduce the generation of emissions in transient states. The logic is verified for sloped load and variable engine speed conditions

2. CONTROL SYSTEM

2.1. Combustion Analysis

The control system consists of a combustion analysis part and a combustion control part. Within the combustion analysis, heat release rate and the MFB50 were calculated using in-cylinder pressure and ECU information. The in-cylinder pressure signals were acquired from each cylinder at a sampling rate of 20 kHz, as well as crank position sensor data. The received time base pressure signals were regenerated for the crank angle base signal using linear interpolation for every 1° CA. The ECU information was corrected in the combustion control part by ETK communiation and transmitted by CAN to the combustion analysis part. The pressure signals were pegged with an intake manifold pressure of ECU information. Then, the heat release rate was calculated using Equation (1) and added together to determine the total heat release rate from the injected fuel. The MFB50 was determined by calculating the crank angle when half of the total heat was released. The heat transfer to the cylinder walls and pistons were ignored (Heywood, 1988).

$$\frac{dQ_{ch}}{d\theta} = \frac{\gamma}{\gamma-1} p \frac{dV}{d\theta} + \frac{1}{\gamma-1} V \frac{dp}{d\theta} \quad (1)$$

To extract the analyzed combustion data for each cylinder in real-time, the calculation process must be executed in sequence with an optimized plan. The injection control strategy should be prepared prior to the BDC because of the time required for overwriting in the ECU. Considering the time requirements of the control logic calculation and data transfer, combustion analysis should be completed by the end of each cycle. To overcome this limited time frame, the calculation window for the heat release calculation should be narrowed and the start of the calculation should be earlier. The rate of heat release was calculated using data from 40° CA BTDC to 90° CA ATDC. The detailed process schedules is shown in Figure 1. All calculations of combustion reaction parameters were finished before 360° CA ATDC (Yu *et al*., 2013).

2.2. Combustion Control Algorithm

The MFB50 which was calculated in the combustion analysis part was provided as feedback for the closed loop combustion control system. The MFB50 of the last cycle was transmitted to the combustion control part through CAN bus after 360° CA ATDC. The MFB50 was compared with the target value at the present operating condition, and the difference was calculated. In order to minimize differences, the PID controller component changed the engine operating parameters by adding correction value to the current engine operating parameters in the ECU. Finally, these values are sent back to the ECU again and the ECU uses these values for the engine operation. In addition, a calibration factor was used to include changes caused by the coolant temperature, environment and other external factors so that the precise target value could be set and controlled. Figure 2 shows a schematic diagram of the combustion control algorithm and combustioqn analysis.

The target map of the MFB50 consisted of a lookup table with an engine speed axis and a fueling rate axis. The values of the table were determined on the basis of the steady-state experimental results. The target MFB50 was determined by linear interpolation according to the current engine speed and the fuel injection rate. The engine speed and fueling rate were recieved from ECU by ETK communications. In addition, a calibration factor was added to compensate changes in the coolant temperature that caused the combustion characteristics to vary. To minimize

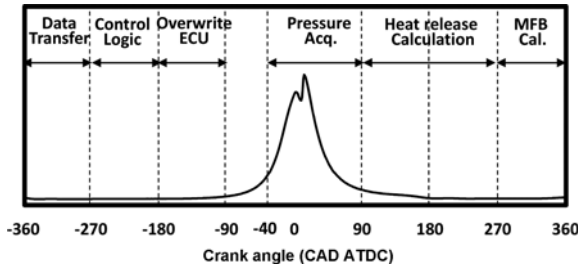

Figure 1. Timing schedule of the combustion analyzer and controller.

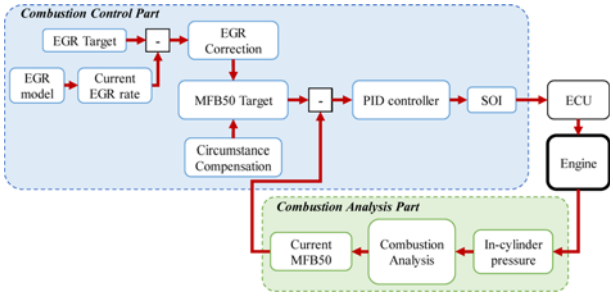

Figure 2. Schematic diagram of the combustion control system.

differences between the targeted and measured values, the main injection timing was adjusted. The corrected main injection timing was determined from PID controller. The value was overwriten to the current main injection timing of ECU.

The MFB50 control were very effective in emitting soot during the transient state (Yu *et al*., 2013). Emission caused by injector failure could be restrained. However, when less EGR gas was trapped in cylinders during the transient state than steady state, the NOx emission increased. If the current MFB50 was controlled to follow the target MFB50 determined from the steady state experiment, the control was not effective in reducing NOx emissions. To counter these problems for the MFB50 control, the correlation factor for the MFB50 target was determined by the EGR rate. The correction factor was activated when the estimated EGR rate was lower than the target EGR rate. The current EGR rate could be estimated in real-time by measuring the in-cylinder pressures and estimating the temperature of gas trapped in the cylinders. Higher NOx emission was expected when the actual EGR rate was lower than the target EGR rate measured during steady state. The most effective way to reduce NOx emissions using an injection strategy was to retard the main injection timing. However, the retarding of main injection timing was limited to prevent loss of IMEP and combustion instability. The target EGR was determined by subtracting the margin value from an EGR rate map to maintain low-level NOx emissions, particularly during transient states (Hong, 2008).

3. EGR MODEL

The EGR prediction model was based on the ideal gas equation of state. The total mass of the in-cylinder gas at IVC can be derived using the pressure, volume, gas constant and temperature of the in-cylinder gas. The mass of the EGR gas can be calculated if the mass of fresh air and the mass of the residual gas are known. For combustion analysis, the in-cylinder pressure was measured by pressure sensors, and the in-cylinder volume at IVC can be easily calculated. The mass of the fresh air per cycle was measured by the ECU. As the control logic and the ECU communicated with each other using ETK communication,

the EGR model received the mass of the fresh air from the ECU.

The temperature of the in-cylinder gas at IVC was calculated using the ideal gas equation. The temperature could be easily derived using the energy conservation equation, neglecting heat transfer from the cylinder wall to the gas. However, heat transfer was not negligible. Prior literature has used a correction factor to remove the error; however, these correction factors were not based on thermodynamic or fluid dynamic principles. In this model, the primary source of error was minimized by considering heat transfer effect with three assumptions;

(1) There is no heat transfer in the intake manifold because it is too small compared to the heat transfer in the cylinder.
(2) The residual gas fraction is fixed to a constant.
(3) The cooling efficiency of the EGR cooler is constant (Heywood, 1988).

3.1. Overall of Model

According to the gas equation of state, the mass of the in-cylinder gas at IVC is calculated as Equation (2), where P_{IVC}, V_{IVC}, T_{IVC} and m_{IVC} represent pressure, volume, temperature and mass in the cylinder at IVC. The pressure at IVC was measured using the installed in-cylinder pressure sensor.

$$\frac{P_{IVC}V_{IVC}}{RT_{IVC}} = m_{IVC} \tag{2}$$

The mass of the gas in a cylinder at IVC was calculated using the mass of the fresh air, the mass of the EGR gas and the mass of the residual gas as shown Equation (3). The fresh air flow rate per cylinder was measured by using the HFM, and this measured value was provided for the model in real time.

$$m_{IVC} = m_{air} + m_{EGR} + m_{RG} \tag{3}$$

The mass of the residual gas was removed using Equations (4) and (5), where RGF is the ratio of the mass of residual gas trapped inside the cylinder.

$$RGF(\%) = \frac{m_{RG}}{m_{air} + m_{EGR} + m_{RG}} \times 100 \tag{4}$$

$$m_{RG} = \frac{RGF}{100 - RGF}(m_{air} + m_{EGR}) \tag{5}$$

If heat losses are neglected, the law of conservation of energy is applicable to the temperature, $T_{IVC,noHT}$, at IVC as Equation (6).

$$C_{IVC}T_{IVC,noHT}m_{IVC} = C_{air}m_{air}T_{air} + C_{EGR}m_{EGR}T_{EGR} + C_{RG}m_{RG}T_{RG} \tag{6}$$

The molar specific heats of fresh air, the EGR, and residual gases are approximately equal, so they are removed from Equation (6) (Kang and Farrell, 2005). Thus, $T_{IVC,noHT}$ is able to be represented as Equation (7).

$$T_{IVC,noHT} = \frac{T_{air}m_{air} + T_{EGR}m_{EGR} + T_{RG}m_{RG}}{m_{air} + m_{EGR} + m_{RG}} \tag{7}$$

However, the heat transfer from the in-cylinder walls to the in-cylinder gas is not negligible. A term representing the increased gas temperature due to this heat transfer is applied to the Equations (8) and (9).

$$T_{IVC} = T_{IVC,noHT} + \Delta T_{IVC,HT} = T_{IVC,noHT} \times \eta_{HT} \tag{8}$$

$$\eta_{HT} = \frac{T_{IVC}}{T_{IVC,noHT}} = 1 + \frac{\Delta T_{IVC,HT}}{T_{IVC,noHT}} \tag{9}$$

Combining Equations (5), (7) and (9), the mass of the EGR gas is calculated as Equation (10).

$$m_{EGR} = \frac{\frac{P_{IVC}v_{IVC}}{R\eta_{HT}} - m_{air}(T_{air} + T_{RG} \times \frac{RGF}{100 - RGF})}{T_{EGR} + T_{RG} \times \frac{RGF}{100 - RGF}} \tag{10}$$

The EGR rate is then calculated as Equation (11).

$$EGR(\%) = \frac{m_{EGR}}{m_{air} + m_{EGR}} \times 100 \tag{11}$$

The EGR rate calculation was scheduled to be complete during the intake stroke. Then the calculated EGR rate was used to control the injection strategy.

3.2. Sub-part Calculation

The variation of the residual gas in a CI engine is relatively narrow compared to that of an SI engine, and the average amount of residual gas in a CI engine is lower than that in an SI engine. In this study, the residual gas fraction, RGF, was assumed as a constant fixed at 3.11 %. Using the variables EGR and RGF, Equation (7) is re-defined as Equation (12), where EGR_{n-1} is the EGR rate of the previous cycle.

$$T_{IVC,noHT} = \frac{T_{intercooler} \times (100 - EGR_{n-1}) + T_{EGR} \times EGR_{n-1}}{100} \times \frac{100 - RGF}{100} + T_{RG} \times \frac{RGF}{100} \tag{12}$$

The convective heat transfer from the cylinder wall to the in-cylinder gas is calculated as Equation (13), where h_c, A_{eff}, A_{piston}, A_{liner} and A_{head} are the convection coefficient, effective area, area of piston, area of liner and area of head

$$\frac{dQ}{dt} = h_c \sum A_{eff}(T_{wall} - T_{cyl}) = h_c[A_{piston}(T_{piston} - T_{cyl}) + A_{liner}(T_{liner} - T_{cyl}) + A_{head}(T_{head} - T_{cyl})] \tag{13}$$

The area of the liner is considered to be the averaged liner area for every crank angle from BDC to IVC. The area of the piston is considered to be 1.3 times larger than the area of the head.

The convection coefficient, h_c, is defined by Woschni's correlation (Park, 2009), Equation (14), where B is the bore of the target engine. The pressure at the intake stroke, p, is

defined as the boost pressure, and the temperature at the intake stroke, T, is defined as the intake manifold temperature.

$$h_c = 3.26B^{-0.2} p^{0.8} T^{-0.55} w^{0.8} \quad (14)$$

The average cylinder gas velocity, w, was determined for a 4-stroke direct injection CI engine when the gas exchange period is expressed as Equation (15).

$$w = C_1 \bar{S}_p \quad (15)$$

For the gas exchange period, C1 is 6.18. The total convective heat transfer in the intake stroke is calculated as Equation (16).

$$Q = \frac{dQ}{dt} \times T_{BDC\sim IVC} \quad (16)$$

The duration of the heat transfer, BTDC ~ IVC, is considered to be the time from BDC to IVC.

The transferred heat cause the in-cylinder gas temperature to increase. This increased temperature is calculated as Equation (17), where C_V is the specific heat at constant volume and m is the mass of the in-cylinder gas at IVC.

$$\Delta T_{IVC,HT} = \frac{Q}{C_v m_{in\text{-}cylinder}} \quad (17)$$

The temperature of the fresh air downstream of the intercooler is calculated using a lookup table. The temperature is then determined in accordance with the engine speed and the total injected fuel mass per cycle.

$$T_{air} = f(RPM, m_{fuel}) \quad (18)$$

The temperature of the exhaust gas is derived from the second order polynomial equation of the total injected fuel mass. Equation (19) was derived from results which were measured in an exhaust manifold for 49 engine operating conditions, varying load and speed in steady state. The coefficient of determination was 0.992.

$$T_{exhaust} = C_1 \cdot m_{fuel}^{\ 2} + C_2 \cdot m_{fuel} + C_3 \quad (19)$$

The temperature of the EGR gas after the EGR cooler is derived as Equations (20) and (21).

$$\eta_{EGRcooler}(\%) = \frac{T_{exhaust} - T_{EGR}}{T_{exhaust} - T_{coolant}} \times 100 \quad (20)$$

$$T_{EGR} = T_{exhaust} - \frac{\eta_{EGRcooler}}{100} \times (T_{exhaust} - T_{coolant}) \quad (21)$$

$\eta_{EGRcooler}$ is the cooling efficiency of the EGR cooler. In this study, the efficiency was fixed to 88 %, which was the average of the results for representative engine operating conditions when the EGR is activated.

4. EXPERIMENTAL SETUP

The engine and the control system were operated with an AVL dynamometer system. A Horiba MEXA-7100DEGR exhaust gas analyzer was used to measure NOx, HC and CO. An AVL gravity-type fuel flow meter measured fuel consumption rate. The engine coolant and fuel temperatures were controlled to 85 °C and 40 °C respectively.

Table 1. Specifications of the target engine.

Criteria	Specification
Engine type	In-line 4 cylinder
Displacement volume	2.2 liter
Maximum power	200 hp / 3800 rpm
Maximum torque	44.5 kgm / 1800 ~ 2500 rpm
Bore	85.4 mm
Stroke	96.0 mm
Compression ratio	16.0

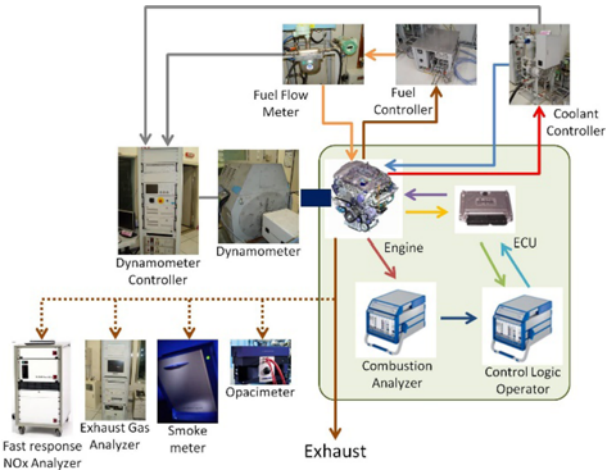

Figure 3. Schematic diagram of the engine test and measurement equipment.

The developed combustion analysis and control algorithm were validated by engine tests. The real-time control system setup and other measurement equipment are shown in Figure 3. A 2.2 L conventional engine with four cylinders was used in this research. Specification of the engine is described in Table 1. One of the ES-1000s was used to the combustion analysis, while the other was used to operate the control algorithm and estimate the EGR rate. To measure the in-cylinder pressure in real-time, glow-plug-type pressure sensors manufactured by Beru were used. Pressure measurement signals of four cylinders were collected using the piezo-resistive method, which had a measuring range of 0 ~ 200 bar.

5. EXPERIMENTAL RESULTS

5.1. EGR Model Verification

The EGR rate model was verified for various engine-operating conditions through the engine test. The EGR rate

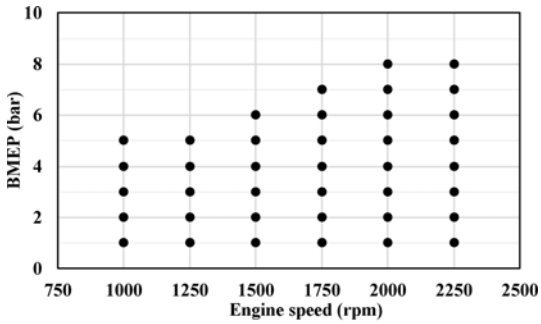

Figure 4. Test conditions for verification of the EGR rate model.

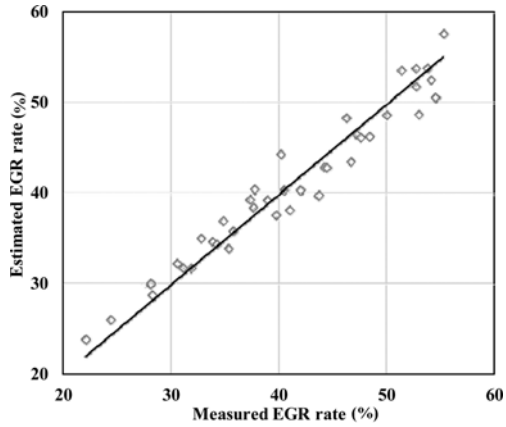

Figure 5. Varification of the EGR rate estimation model.

was measured at steady state operating conditions when the exhaust gas temperature and engine oil temperature reached a steady state value. The EGR rate was measured by the exhaust emission analyzer, simultaneously, the estimated EGR rate was calculated through the EGR model using the ES1000. The response of the gas analyzer was not fast enough to measure behavior of the EGR rate during a transient operation, the model was verified for steady state conditions. The test conditions are shown in Figure 4. The x-axes and y-axes correspond to engine speed and engine BMEP, respectively. Measured and estimated EGR rates are compared in Figure 5. The x- axes and y- axes correspond to the measured and estimated EGR rates, respectively. The coefficient of determination was 0.9397, showing good agreement between the measured and estimated data.

5.2. Emission Characteristics in the Transient State with Combustion Control Using the EGR Model

When the engine speed and load were during the transient operation, the air and EGR supply system showed a time lag. This caused the EGR rate to not be maintained in the same way as during steady state conditions. This time lag caused undesirable in-cylinder gas conditions. This phenomenon was caused by the delay of the boost pressure and the EGR supply. The actual boost pressure was always

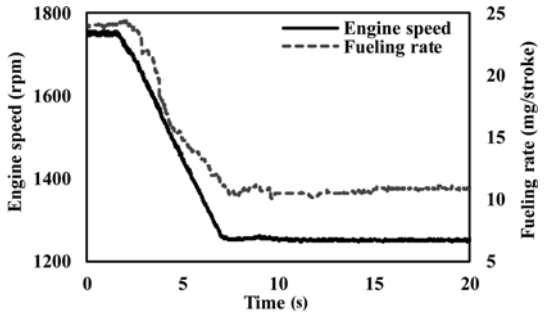

Figure 6. Engine speed and load in transient state.

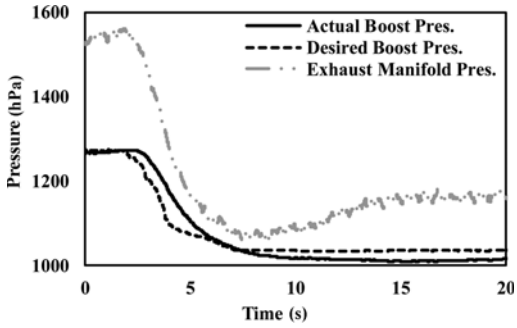

Figure 7. Behavior of boost pressure and exhaust manifold pressure.

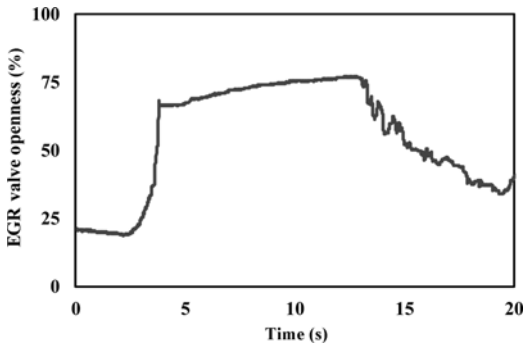

Figure 8. Behavior of EGR valve openness.

slower than the target boost pressure during transient conditions because of the inertia of the turbocharged turbine and compressor. For example, if the engine speed and load abruptly decreased, the decline of the actual boost pressure was always slower than the decline of the target boost pressure. The engine speed and load were decreased from 1750 rpm to 1250 rpm, and BMEP from 5 bar to 1 bar for 5 seconds (Figure 6). The EGR gas flow rate was determined by the difference between the exhaust manifold pressure, the intake manifold pressure and the effective EGR valve area. When the engine load decreased, the exhaust gas pressure dropped as quickly as the decrease in the fuel injection quantity. However, the decrease of the intake manifold pressure was slower than that of the exhaust manifold pressure as shown in Figure 7. This slower decrease blocked the supply of the EGR gas to the

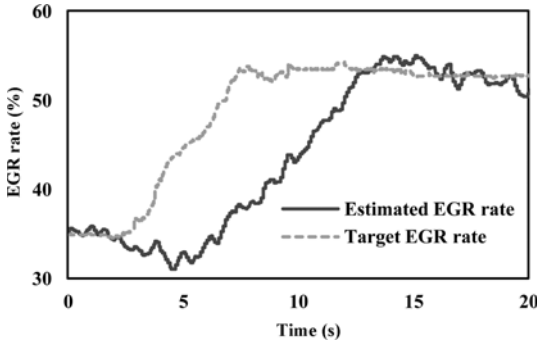

Figure 9. Behavior of target EGR rate and estimated EGR rate when engine speed and load decrease.

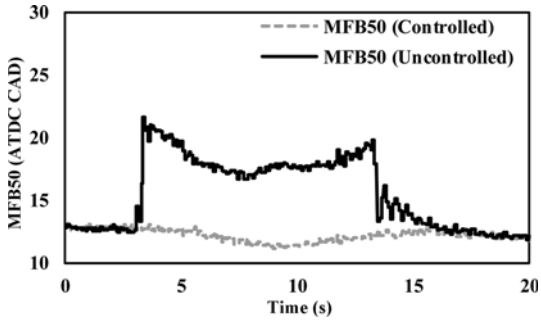

Figure 10. Behavior MFB50 when the control is applied.

intake manifold, even though the EGR valve was widely opened (Figure 8). A higher EGR rate was required when a lower load was required by the engine. However, when the engine experiences a sudden decrease in the engine load, the engine will be starving for EGR gas because of the above phenomenon. The estimated EGR rate and target EGR rate were shown in Figure 9. The target map of the EGR rate consisted of a lookup table with an engine speed axis and a fueling rate axis. The values of the table were determined on the basis of the steady-state experimental results. The target EGR rate was determined by linear interpolation according to the current engine speed and the fuel injection rate. Engine-out NO emissions showed a

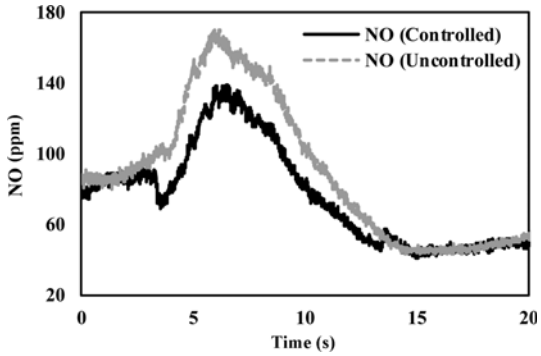

Figure 11. Behavior NO emission when the control is applied.

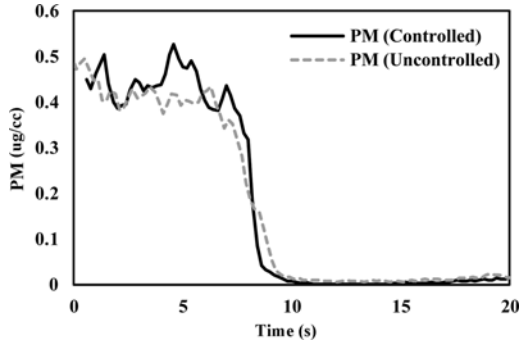

Figure 12. Behavior PM emission when the control is applied.

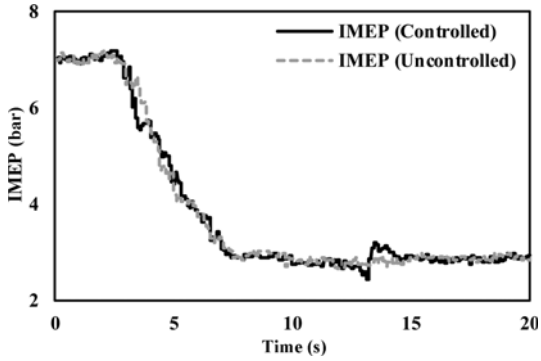

Figure 13. Behavior IMEP when the control is applied.

peak at this state, as shown in Figure 11. One possible solution is to adjust the injection strategy to the actual EGR rate. As described by MFB50 control logic, the target MFB50 was retarded when the actual EGR rate was lower than the target EGR rate.

When the engine speed and load decreased, the gap between the target and actual EGR rate increased. However, the main injection timing was retarded because of the retarded target MFB50. The behavior was shown in the Figure 10. The NO emission peak was also reduced, unlike what occurred in the case without the control as shown in Figure 11. Controlling the MFB50 with the EGR rate model was effective for maintaining low-level NO emissions during the transient state. The PM emission level was not increased and the IMEP was not reduced (Figures 12 and 13).

6. CONCLUSION

An EGR rate prediction model was developed based on the ideal gas equation of state. Input data were acquired from ECU variables and the cylinder pressure was measured. The EGR rate model was verified for several engine operating conditions. The results showed meaningful agreement between the measured and estimated data.

The effect of combustion control logic using the EGR rate model was tested during a transient operation. The

correction factor derived by the EGR rate had an effect on the reduction of the NOx emission peak during the transient state when the engine speed and load decrease. The target MFB50 was retarded when the estimated EGR rate was lower than the target EGR rate, as determined by steady state experiments. The main injection timing was retarded to follow the modified target MFB50, and the NOx emission peak during a deceleration state was reduced as a result of the retarded main injection timing.

ACKNOWLEDGEMENT−This research was supported by the Institute of Advanced Machinery and Design at Seoul National University.

REFERENCES

Audi Diesel Targets Bin 5, Euro 6 (2015). http://www.sae.org/automag/technewsletter/080129DieselTech/04.htm

Guillemin, F., Grodin, O., Chauvin, J. and Nguyen, E. (2008). Combustion parameters estimation based on knock sensor for control purpose using dedicated signal processing platform. *SAE Paper No*. 2008-01-0790.

Hasegawa, M., Shimasaki, Y., Yamaguchi, S., Kobayashi, M., Sakamoto, H., Kitayama, N. and Kanda, T. (2006). Study on ignition timing control for diesel engines using in-cylinder pressure sensor. *SAE Paper No*. 2006-01-0180.

Hagena, J. R., Filipi, Z. S. and Assanis, D. N. (2006). Transient diesel emissions: Analysis of engine operation during a tip-in. *SAE Paper No*. 2006-01-1151.

Hong, K. (2008). *A Study on the Effect of Multiple Injection on Common Rail HSDI Diesel Engine Performance and Emissions*. M. S. Thesis. Seoul National University. Seoul, Korea.

Heywood, J. B. (1988). *Internal Combustion Engine Fundamentals*. 2nd edn. Mc-GrawHill. New York, USA.

Husted, H., Kruger, D., Fattic, G., Ripley, G. and Kelly, E. (2007). Cylinder pressure-based control of pre-mixed diesel combustion. *SAE Paper No*. 2007-01-0773.

Honda Prepares i-DTEC Diesel for 2009 (2015). http://www.sae.org/automag/technewsletter/080129DieselTech/01.htm

Kirchen, P., Obrecht, P. and Boulouchos, K. (2009). Soot emission measurements and validation of a mean value soot model for common-rail diesel engines during transient operation. *SAE Paper No*. 2009-01-1904.

Kang, H. and Farrell, P. V. (2005). Experimental investigation of transient emissions (HC and NOx) in a high speed direct injection (HSDI) diesel engine. *SAE Paper No*. 2005-01-3883.

Kumar, R., Zheng, M., Asad, U. and Reader, G. (2007). Heat release based adaptive control to improve low temperature diesel engine combustion. *SAE Paper No*. 2007-01-0771.

Liebig, D., Krane, W., Ziman, P., Garbe, T. and Hoenig, M. (2008). The response of a closed loop controlled diesel engine on fuel variation. *SAE Paper No*. 2008-01-2471.

New GM V6 Diesel Has Cylinder-pressure Monitoring (2015). http://www.sae.org/automag/technewsletter/070402Powertrain/01.htm

Ohyama, Y. (2001). Engine control using combustion model. *Int. J. Automotive Technology* **2**, **2**, 53−62.

Park, Y. (2009). *Mean Value Air Path Modeling for High Speed Direct Injection Diesel Engine Equipped with VGT and EGR*. M. S. Thesis. Hanyang University. Seoul, Korea.

Punater, A., Ripley, G. and Schten, K. (2008). Controller for rapid development of advanced mode combustion algorithm using cylinder pressure feedback. *Convergence Transportation Electronics Association*.

Reitz, R. and Ehe, von der J. (2006). Use of in-cylinder pressure measurement and the response surface method for combustion feedback control in a diesel engine. *IMechE Part D: J. Automobile Engineering* **220**, **11**, 1657−1666.

Schnorbus, T., Pischinger, S., Korfer, T., Lamping, M., Tomazic, D. and Tatur, M. (2008). Diesel combustion control with closed-loop control of the injection strategy. *SAE Paper No*. 2008-01-0651.

VW Jetta SportWagen Scores High (2008). http://www.greencar.com/articles/vw-jetta-sportwagen-scores-high.php

Willems, F., Doosje, E., Engels, F. and Seykens, X. (2010). Cylinder pressure-based control in heavy-duty EGR diesel engines using a virtual heat release and emission sensor. *SAE Paper No*. 2010-01-0564.

Yoon, M., Lee, K. and Sunwoo, M. (2007). A method for combustion phasing control using cylinder pressure measurement in a CRDI diesel engine. *Mechatronics* **17**, **9**, 469–479.

Yu, S., Choi, H., Cho, S., Han, K. and Min, K. (2013). Development of engine control using the in-cylinder pressure signal in a high speed direct injection diesel engine. *Int. J. Automotive Technology* **14**, **2**, 175−182.